Research Square

Preprints are preliminary reports that have not undergone peer review.
They should not be considered conclusive, used to inform clinical practice,
or referenced by the media as validated information.

Trees and Restoration Part of a collection:Drought stress Trait adjustments of two precious timber tree species to mixed planting in subtropical karst rocky desertification area

Chunyan Wan
Guangxi University
Yuanguang Wen
Guangxi Academy of Sciences
Xiaoguo Zhou
Guangxi Academy of Sciences
Shidan Zhu
zhushidan@gxu.edu.cn
Guangxi University

Research Article

Keywords: Hydraulic safety, Karst, Mixed stands, Nutrient efficiency, Restoration, Strategy

Posted Date: November 27th, 2026

DOI: https://doi.org/10.21203/rs.3.rs-11509930/v1

License: This work is licensed under a Creative Commons Attribution 4.0 International License.
Read Full License

Additional Declarations: No competing interests reported.

Trees and Restoration

Part of a collection:Drought stress

Trait adjustments of two precious timber tree species to mixed planting in subtropical karst rocky desertification area

Chunyan Wan[1,2], Yuanguang Wen[3], Xiaoguo Zhou[3], Shidan Zhu[1,2]*

[1]*Guangxi Key Laboratory of Forest Ecology and Conservation, School of Forestry, Guangxi University, Daxuedong Road 100, Nanning 530004, Guangxi, China*

[2]*Guangxi Shiwandashan Forest Ecosystem Position Observation and Research Station, Fangcheng District, Fangchenggang 538021, Guangxi, China*

[3]*Institute of Ecological Industry, Guangxi Academy of Sciences, Daling Road 98, Nanning 530003, Guangxi, China*

[*]**Corresponding author:**

Shi-Dan Zhu

Email: zhushidan@gxu.edu.cn

Tel: +86-0771-3185847

ORCID

Chunyan Wan: https://orcid.org/0009-0009-1577-0765

Shidan Zhu: https://orcid.org/0000-0002-9228-368X

Abstract

Afforestation has long been a major challenge in karst rocky desertification (KRD) areas because of severe water and nutrient limitation. Developing precious timber plantations is considered an effective way for KRD restoration. Hence, there is an urgent need to understand the eco-physiological adaptation of timber tree species to KRD environment and afforestation models. This study was conducted on an afforestation experimental platform established in 2011 in a subtropical KRD area. We investigated growth, cumulative mortality, hydraulic traits, carbon isotope composition ($\delta^{13}C$), nutrient concentrations and resorption efficiencies of two Fabaceae timber species (*Dalbergia odorifera* and *Acrocarpus fraxinifolius*) from their monocultures and mixed stand (1:1) in 2024. The main objective of this study was to clarify the differences in growth and mortality between monocultures and mixed stand and the underlying physiological mechanisms. Our results showed that regardless of afforestation models cumulative mortality of both species remained below 25% after 13 years, during which three extreme drought episodes occurred. Compared to respective monoculture, *D. odorifera* in mixed stand exhibited higher leaf mass per area, stem saturated water content, minimum leaf water potential, and hydraulic safety margin, which were associated with lower cumulative mortality. By contrast, *A. fraxinifolius* in mixed stand had higher leaf N, lower $\delta^{13}C$ and N and P resorption efficiencies than in monoculture. The enhanced resource-acquisitive strategy contributed to faster growth in mixed stand. This study reveals that species-specific trait adjustments explain the variations of growth and mortality between monoculture and mixed stand, which should be considered for afforestation species selection and mixed stand design in KRD regions.

Keywords: Hydraulic safety, Karst, Mixed stands, Nutrient efficiency, Restoration, Strategy

Introduction

The Southwest China Karst, one of the world's largest contiguous karst areas, has been confronting the issue of karst rocky desertification (KRD; Wang et al. 2004; Yang et al. 2025; Su et al. 2026). To restore degraded karst ecosystems, large-scale ecological restoration programs have been implemented in recent decades (Qiu et al. 2022; Yue et al. 2022). Remote-sensing analyses indicate a significant expansion of vegetation greening area in the region; however, many plantations have low stability and survival under severe droughts (Zhao and Hou, 2019; He et al. 2022; Zhong et al. 2022; Yue et al. 2024). The difficulties of KRD restoration are mainly caused by extremely adverse environmental conditions, including extensive bedrock exposure, shallow and discontinuous soils, rapid water loss, and nutrient imbalance (Jiang et al. 2014; Li et al. 2023). These environmental limitations impose strong constraints on plants' water and nutrient acquisition and consequently on their growth and mortality. Therefore, understanding the eco-physiological adaptation of afforestation tree species is essential for developing sustainable plantations in KRD areas.

Functional traits are commonly used to explore plants' adaptation to environmental stress (Wright et al. 2004; Díaz et al. 2016; Li and Prentice, 2024). Economic traits, such as leaf mass per area (LMA) and wood density (WD), reflect the structural investment in leaves and stems, respectively. Higher LMA and WD are generally associated with more conservative resource-use strategies and lower growth rates (Wright et al. 2004; Chave et al. 2009). Hydraulic traits characterize the capacity of plants to transport water and withstand drought-induced hydraulic dysfunction (Meinzer et al. 2009; Choat et al. 2012; Torres-Ruiz et al. 2024). Xylem embolism resistance is commonly represented by the water potential causing 50% and 88% losses of hydraulic conductivity (P_{50} and P_{88}), which also reflects the threshold of hydraulic failure (Choat et al. 2012; Urli et al. 2013). Hydraulic safety margin (HSM) indicates the distance between the minimum water potentials

experienced by plants and P_{50} (or P_{88}), reflecting the degree of drought-induced hydraulic failure (Choat et al. 2012; Delzon and Cochard, 2014; Anderegg et al. 2016). Leaf and stem water storage can buffer short-term imbalances between water supply and transpirational demand during drought periods (Luo et al. 2021; Salomón et al. 2024). Carbon isotope composition ($\delta^{13}C$) integrates long-term variation in carbon assimilation and stomatal regulation and is widely used as an indicator of water use efficiency (Cernusak et al. 2013; Busch et al. 2020; Ma et al. 2023). Leaf nutrient concentrations and stoichiometric ratios reflect plant nutrient status and limitation, and nutrient resorption efficiencies indicate the capacity to conserve and recycle nutrients before leaf senescence (Vergutz et al. 2012; Zhang et al. 2024). These economic, hydraulic, and nutrient traits have been widely evaluated to characterize stress resistance and growth potential of afforestation tree species, thereby informing species selection and plantation management (Zhu et al. 2018; Wang et al. 2021; Guimarães et al. 2026). We therefore expect these traits are particularly important for explaining the performance of tree species planted in KRD areas with concurrent water and nutrient limitations.

Functional traits can vary within a given plant species, reflecting phenotypic responses to various environmental conditions (Albert et al. 2010; Siefert et al. 2015; Westerband et al. 2021). Such trait adjustment is ecologically important, because it affects growth, persistence, and species coexistence (Turcotte and Levine, 2016; Pérez-Ramos et al. 2019). Recently, much attention has been paid to intra-specific trait variation between monoculture and mixed stand differing distinctly in canopy structure and resource availability. This is because trait plasticity could reduce niche overlap, thus improving tree persistence and stand productivity (Kunstler et al. 2016; Fichtner et al. 2018). For example, compared to monoculture, leaf N of European beech (*Fagus sylvatica*) increases when mixed with sessile oak (*Quercus petraea*) but decreases when mixed with Norway spruce (*Picea abies*), whereas Norway spruce exhibits limited traits variations across different stand types (Serrano-León et al. 2022). In another study, a meta-analysis of 43 studies revealed that seven of the eight

examined leaf traits showed significant intra-specific differences between monocultures and mixed stands, with LMA and leaf N exhibiting the strongest responses (Felix et al. 2023). Therefore, exploring the magnitude and direction of trait variation across stand types can help identify compatible species combinations in mixed stands.

Fabaceae tree species have long been used in ecological restoration worldwide (Kettle, 2012; Pereira et al. 2013). Many Fabaceae species form symbiotic associations with N-fixing rhizobia, which can increase soil N availability and facilitate vegetation recovery in nutrient-poor environments (Forrester et al. 2005; Menge and Hedin, 2009). In addition, some Fabaceae species also show strong drought tolerance through deep rooting, effective stomatal regulation, and conservative water-use strategies, contributing to strong adaptation to water-limited habitats (Pineda-García et al. 2013; Xiang et al. 2021a; Feng et al. 2022). Furthermore, several Fabaceae tree species (e.g., *Dalbergia* and *Acrocarpus*) produce high-value timber, which has been widely used for cultivating large-diameter precious timber plantations (Sun et al. 2015). Due to the aforementioned ecological and economic benefits, an afforestation trial was conducted using two Fabaceae timber tree species (*Dalbergia odorifera* and *Acrocarpus fraxinifolius*) in a subtropical KRD area in 2011. Here, we investigated growth and cumulative mortality of the two species in their monocultures and mixed stand, and measured LMA, WD, hydraulic traits, saturated water content, $\delta^{13}C$, leaf nutrients, N and P resorption efficiencies. We aimed to address the following two questions: (1) How do the growth and cumulative mortality of the two species differ between monoculture and mixed stand? and (2) Are these demographic changes associated with variations in hydraulic and nutrient-use strategies? By linking trait adjustments to restoration performance, this study will provide useful insights for developing precious timber plantations in KRD areas.

Materials and methods

107 **Study site and plant materials**

108 This study was conducted in the Forest Restoration Experimental Platform (23°24′–24°20′ N, 107°41′–
109 108°29′ E) established in a typical rocky desertification area in Mashan County, central Guangxi (Fig. 1). The
110 study site is a typical karst peak-cluster depression landscape, with elevations ranging from 250 to 450 m and
111 slopes between 25° and 35°. The region is influenced by a subtropical monsoon climate (Wang et al. 2004).
112 The mean annual temperature is 21.3°C, with monthly mean temperatures ranging from 12.5°C in January to
113 28.4°C in July (Jiang et al. 2014). Mean annual precipitation is 1667 mm, and more than 76% of the annual
114 precipitation occurs during the rainy season from May to October (Liu et al. 2018). The geological substrate
115 consists of Devonian to Permian carbonate rocks, primarily limestone and dolomite (Zhang et al. 2015). The
116 dominant soil type is limestone-derived soil, which is neutral to slightly alkaline, with a pH of 7.2–7.8, organic
117 matter content of 1.5–3.0%, and available phosphorus concentrations of 2.1–4.5 mg kg^{-1}.

118 Due to long-term human disturbances, including excessive land reclamation, fuelwood collection, and
119 grazing, the original subtropical evergreen broad-leaved forests in the region have largely disappeared. The
120 current vegetation is dominated by secondary shrublands and herbaceous communities (Li et al. 2022). Mashan
121 County is located within the Southwest China rocky desertification control zone identified in China's national
122 ecological restoration planning and is an important area for rocky desertification control and vegetation
123 restoration (National Development and Reform Commission, 2013). The experimental plantation was
124 established in March 2011 using a randomized complete block design, with five blocks distributed across
125 approximately 6 ha. Within each block, one 20 m × 20 m plot was established for each stand type, resulting
126 in five replicate plots per stand type. Three stand types were established: a *D. odorifera* monoculture, an *A.*
127 *fraxinifolius* monoculture, and a mixed stand of *D. odorifera* and *A. fraxinifolius* at an initial planting ratio of
128 1:1. Each plot was treated as an independent experimental unit. The experimental plots were selected to ensure

comparability in elevation, slope, aspect, soil type, and land-use history, thereby minimizing potential confounding effects associated with site conditions. Most plant sampling and functional-trait measurements were conducted during the rainy season from May to September 2024 to minimize the influence of short-term water limitation and ensure seasonal comparability among stand types. Midday leaf water potential was monitored across seasons, and the lowest recorded value was defined as Ψ_{min}. Functional-trait sampling was conducted across all five replicate plots of each stand type. Measurements obtained from multiple organs of the same tree were first averaged at the individual-tree level, and the resulting individual-tree values were subsequently averaged within each plot to obtain plot-level means for statistical analyses.

Growth rate and cumulative mortality

Growth was measured in 2024, 13 years after plantation establishment. The diameter at breast height (DBH) of every surviving tree in each sample plot was recorded. Because initial DBH measurements were unavailable, growth was quantified as the annual DBH increment since plantation establishment:

$$Growth = \frac{DBH_t}{A_t}$$

where DBH_t is the DBH of an individual surviving tree measured in 2024, and A_t is the plantation age at measurement, equal to 13 years. For each plot, the mean annual DBH increment was calculated by averaging the values of all surviving individuals of each species.

Tree cumulative mortality was surveyed in 2011, 2013, and 2024. Dead individuals were identified from remaining stems, fixed planting positions, and the original planting records. Cumulative mortality at census (t) was calculated as:

$$\text{Cumulative mortality}_t = \frac{N_{initial} - N_t}{N_{initial}} \times 100\%$$

where $N_{initial}$ is the number of individuals initially planted in each plot and N_t is the number of living individuals recorded at census (t). Cumulative mortality at each census was calculated as cumulative mortality

since plantation establishment. Thus, the 2011 and 2013 censuses represented cumulative mortality during the first 8 months and approximately 2 years after planting, respectively, whereas the 2024 census represented cumulative mortality over the first 13 years. Cumulative mortality was calculated separately for each species within each plot.

Leaf hydraulic conductance and vulnerability curves

Branches with leaves were collected from the canopy in the early morning. The cut ends of the branches were wrapped with moist paper towels and then placed in black plastic bags containing additional moist paper towels to maintain hydration, and the branches were rapidly transported to the laboratory. If the leaf water potential was relatively high (> –0.3 MPa), indicating near-saturation, measurements were conducted immediately. If the water potential was lower, a segment was cut underwater and rehydrated for approximately 2 hours before measurements were taken. In this study, the rehydration method was used to measure leaf hydraulic conductance (K_{leaf}) and vulnerability curves (Sack et al. 2003; Yao et al. 2021). The process involved placing the branches in the laboratory and allowing them to naturally dry over different periods to achieve varying water potentials (up to a maximum of 7 days). Before measuring K_{leaf}, the branches were sealed in black plastic bags for at least 1 hour. Subsequently, leaf water potentials at the top and bottom of the branch were measured. If the difference was less than 0.1 MPa, the branch was considered to have reached equilibrium.

After measuring the initial leaf water potential (Ψ_0), two nearby leaves were selected and excised under distilled water, then rehydrated for 10 to 300 seconds. Following rehydration, the leaves were placed in self-sealing bags with moisture-soaked paper towels for 10–60 minutes to achieve equilibrium before measuring the final leaf water potential (Ψ_f). Rehydration was considered complete when Ψ_f approached half of Ψ_0, with longer rehydration and equilibrium times required for more negative Ψ_0 values.

The maximum leaf hydraulic conductance (K_{leaf}) was calculated using the following formula:

$$K_{\mathrm{leaf}} = \mathrm{C} \times \ln\left(\Psi_0/\Psi_f\right)/t$$

where *C* is leaf capacitance and was calculated as follows:

$$\mathrm{C} = \Delta\mathrm{RWC}/\Delta\Psi_1 \times (\mathrm{DM}/\mathrm{LA}) \times (\mathrm{SM}/\mathrm{DM})/\mathrm{M}$$

where DM is the dry mass of leaf (g), LA is the area of leaf, SM is the mass of leaf at water saturation (g), and M is the molar mass of water. $\Delta\mathrm{RWC}/\Delta\Psi_1$ represents the change in leaf relative water content per unit change in water potential. It was derived from the pressure–volume curve obtained by allowing fully hydrated leaves to dry naturally. K_{leaf} at different Ψ_0 values was determined during natural drying, and the relationship was fitted using a sigmoid equation in SigmaPlot 12.5 to construct a leaf vulnerability curve (Fig. S1). The leaf water potential at 88% loss of K_{leaf} ($P88_{\mathrm{leaf}}$) was calculated to characterize the leaf resistance to embolism (Scoffoni et al. 2016; Griffin-Nolan et al. 2023; Matos et al. 2024).

Stem hydraulic conductance and vulnerability curves

The improved bench-drying method was used to construct vulnerability curves of the stem xylem (Sperry et al. 1988; Nolf et al. 2015). Sampling and water potential equilibration followed procedures similar to those used for the leaf vulnerability curves. Upon reaching the desired water potential, the entire stem was wrapped in a plastic bag for 1–2 h to equilibrate. Next, all leaves were removed, and the basal segment of the maximum vessel length (or a node for some species) was cut off under water (Ziegler et al. 2019). The basal incisions of the removed leaves were sealed with glue and Parafilm, and the stem was trimmed and connected to a flow meter (LiquiFlow L13-AAD-11-K-10S, Bronkhorst High-Tech BVA, Netherlands). Utilizing flow analysis programs FlowDDE 4.81 and FlowPlot 3.35, the initial flow rate (J_i) of a 20 mmol L^{-1} KCl solution flowing through the stem under 5 kPa pressure was recorded. The stem was then connected to a flushing device and flushed at 0.20 MPa pressure for 20–30 min until no air bubbles emerged. The maximum flow rate (J_{max}) was measured after flushing. The percentage loss of stem hydraulic conductivity (PLC, %) was calculated as shown

below:

$$\text{PLC}\ (\%) = (1 - J_i/J_{max}) \times 100\%$$

PLC was determined at various xylem water potentials during desiccation. The relationship between Ψ_x and PLC was fitted using the sigmoid equation in SigmaPlot 12.5, and the water potential at 88% loss of stem hydraulic conductivity ($P88_{stem}$) was determined (Fig. S1). In this study, we used P_{88} because it represents a threshold of near-complete xylem hydraulic loss (Choat et al. 2012; Urli et al. 2013; Duan et al. 2022) and is appropriate for assessing hydraulic risk in karst tree species under the extreme drought conditions (Wang et al. 2023).

Minimum leaf water potential and hydraulic safety margins

Minimum leaf water potentials (Ψ_{min}) were measured between 12:00 and 15:00 on consecutive sunny days during the dry season. The hydraulic safety margin (HSM_{88}) was calculated as the difference between Ψ_{min} and $P88$ (Bucci et al. 2019): $HSM_{88} = \Psi_{min} - P88_{stem}$. These values indicate the degree of hydraulic buffering maintained by species before reaching critical thresholds of embolism (Choat et al. 2012).

Leaf mass per area, saturated water content, wood density, and carbon isotope composition

Leaf mass per area (LMA, g m^{-2}) was determined using fully expanded, sun-exposed mature leaves collected during the wet season. For each sampled tree, 20–30 healthy leaves were collected and immediately transported to the laboratory in sealed plastic bags. Fresh leaf area was measured using a leaf area meter or from scanned images. The leaves were then oven-dried at 60°C for 72 h and weighed to obtain leaf dry mass. LMA was calculated as:

$$LMA = \frac{DM_{leaf}}{LA}$$

where DM_{leaf} is leaf dry mass and LA is leaf area.

Leaf saturated water content (SWC_{leaf}; g g^{-1}) was measured using fully expanded, sun-exposed mature

leaves collected during the wet season. For each species, 20–30 healthy leaves were sampled from each individual tree and immediately transported to the laboratory in sealed plastic bags with moist paper to prevent water loss. The leaves were then immersed in distilled water overnight until full saturation. After saturation, leaf surfaces were gently blotted dry with absorbent paper, and the saturated mass (SM_{leaf}, g) was measured using an electronic balance. The leaves were subsequently dried at 60°C for 72 h to obtain dry mass (DM_{leaf}, g). Leaf saturated water content was calculated as:

$$SWC_{\mathrm{leaf}} = \frac{SM_{\mathrm{leaf}} - DM_{\mathrm{leaf}}}{DM_{\mathrm{leaf}}}$$

where SM_{leaf} is the saturated mass of leaves and DM_{leaf} is the leaf dry mass.

Stem saturated water content (SWC_{stem}; g g^{-1}) and wood density (WD) were determined using stem segments collected during the wet season. For each species, five stem segments approximately 5 cm in length and 6–10 mm in diameter were sampled from healthy current-year or sun-exposed branches. After removing the bark and pith with a knife, the wood samples were immersed in water overnight until saturation. The saturated mass (SM_{stem}, g) was measured using a balance (MT204T, Shanghai, China). The volume of the water-saturated wood segment (V, cm^3) was then measured using the water-displacement method (Williamson and Wiemann, 2010). The samples were subsequently dried in an oven at 103°C for 72 h to obtain dry mass (DM_{stem}, g). Wood density (WD; g cm^{-3}) was calculated as the ratio of dry mass to saturated volume:

$$WD = \frac{DM_{\mathrm{stem}}}{V}$$

Stem saturated water content was calculated as:

$$SWC_{\mathrm{stem}} = \frac{SM_{\mathrm{stem}} - DM_{\mathrm{stem}}}{DM_{\mathrm{stem}}}$$

where SM_{stem} is the saturated mass of the stem segment, DM_{stem} is the dry mass of the stem segment, and V is the saturated stem volume.

For carbon isotope analysis, 20–30 fully expanded and sun-exposed leaves were collected from each

sampled tree. Leaf samples were oven-dried at 60°C for 72 h, ground, and passed through a 0.15 mm sieve. The carbon isotope composition of the leaves was determined using an isotope ratio mass spectrometer (Thermo Finnigan MAT DELTAplusXP; Thermo Electron Corporation, MA, USA). Leaf carbon isotope composition ($\delta^{13}C$, ‰) was calculated as:

$$\delta^{13}C = \frac{R_{\text{sample}} - R_{\text{standard}}}{R_{\text{standard}}} \times 1000$$

where R_{sample} and R_{standard} are the $^{13}C/^{12}C$ ratios of the sample and the Pee Dee Belemnite standard, respectively. Leaf $\delta^{13}C$ was used as an integrated indicator of long-term intrinsic water-use efficiency (Da Silveira et al. 1989; Driscoll et al. 2020).

Nutrient concentrations and resorption efficiencies

The collected leaf samples were oven-dried at 80 °C for at least 48 h until constant weight was achieved. Subsequently, the dried leaves were finely ground using a crusher. The resulting powder was used for subsequent measurements of nitrogen, phosphorus, calcium, and magnesium concentrations. Nitrogen concentrations in green leaves (N_{gr}, g kg^{-1}) and senesced leaves (N_{sen}, g kg^{-1}) were determined using a carbon-nitrogen elemental analyzer (Vario MAX CN, Elementar Analysensysteme GmbH, Hanau, Germany). For the determination of phosphorus, calcium, and magnesium concentrations, separate samples were digested with 8 mL of HNO_3 (65–68%) and 4 mL of $HClO_4$ (70–72%). After digestion, the samples were dissolved in 4 mL of HCl (3 M). The concentrations of phosphorus (P_{gr}, P_{sen}, g kg^{-1}) in green and senesced leaves, as well as calcium (Ca, g kg^{-1}) and magnesium (Mg, g kg^{-1}) in green leaves, were analyzed using an inductively coupled plasma atomic emission spectrometer (iCAP 7400, Thermo Fisher Scientific, Bremen, Germany). Nitrogen and phosphorus resorption efficiencies (NRE and PRE, respectively) were calculated using the following formula (Killingbeck, 1996; Vergutz et al. 2012):

$$RE = \left(1 - \frac{Nu_{sen}}{Nu_{gr}} \times MCLF\right) \times 100\%$$

where Nu_{sen} and Nu_{gr} represent the mass-based nutrient concentrations in senesced and green leaves, respectively, and MCLF denotes the mass loss correction factor. The MCLF was calculated as the ratio of the average dry mass of senesced leaves to that of green leaves (Killingbeck, 1996).

Statistical analysis

All statistical analyses were conducted in R version 4.2.2. The effects of stand type (monoculture vs. mixed stand) were analyzed separately for *Dalbergia odorifera* and *Acrocarpus fraxinifolius*. For each variable, measurements obtained from multiple trees or organs within a plot were averaged to obtain a single plot-level value, with the plot treated as the experimental unit. Accordingly, comparisons between stand types were based on five replicate plots per stand type. Differences in functional traits, growth, and cumulative mortality between monocultures and mixed stands were quantified using standardized effect sizes. Principal component analysis (PCA) was performed on standardized plot-level functional-trait values to summarize the major axes of trait variation and to assess multivariate differences between stand types; growth and cumulative mortality were excluded from the PCA. The PCA included 20 plot-level observations (n = 5 plots per species × stand-type combination). Linear regression analyses were used to examine relationships between selected functional traits and annual DBH increment or cumulative mortality. For regressions pooling observations across the two species and two stand types, analyses were based on 20 plot-level observations. Model assumptions were evaluated by inspection of residual diagnostics. All statistical tests were two-tailed, with statistical significance set at $P < 0.05$. All analyses and data visualization were performed in R, with figures generated using the ggplot2 package.

Results

Species-specific functional trait and demographic responses to stand type

The standardized effect sizes revealed distinct species-specific differences in functional traits and demographic performance between monocultures and mixed stands (Fig. 2). *D. odorifera* in mixed stands exhibited significantly higher mean LMA (from 58.08 to 65.28 g m^{-2}), stem saturated water content (SWC_{stem}; from 0.78 to 0.82 g g^{-1}), hydraulic safety margin (HSM_{88}; from 3.55 to 4.29 MPa), and minimum leaf water potential (Ψ_{min}; from −1.77 to −1.42 MPa) than those in monocultures. Cumulative mortality was significantly lower in mixed stands (11.2%) than in monocultures (16.4%), whereas annual DBH increment did not differ significantly between stand types.

For *A. fraxinifolius*, nutrient-use and water-use traits rather than hydraulic traits differed significantly between stand types. Compared with monocultures, mixed stands exhibited significantly higher mean leaf N concentration (from 21.36 to 23.59 mg g^{-1}) and lower NRE (from 53.1% to 47.4%), PRE (from 57.5% to 52.5%), and leaf $\delta^{13}C$ (from −28.86‰ to −30.64‰). Annual DBH increment was 13.1% greater in mixed stands than in monocultures, increasing from 1.02 to 1.15 cm yr^{-1}, whereas cumulative mortality did not differ significantly between stand types.

Principal component analysis

Principal component analysis further revealed contrasting multivariate trait patterns between monocultures and mixed stands (Fig. 3). The first two principal components explained 66.10% of the total trait variation, with PC1 and PC2 accounting for 52.45% and 13.65%, respectively. PC1 primarily represented an axis of structural investment and hydraulic safety. *LMA*, *WD*, Ψ_{min}, and HSM_{88} loaded positively on PC1, whereas SWC_{stem}, $P88_{leaf}$, and $P88_{stem}$ loaded negatively. PC2 primarily represented variation in leaf nutrient status, nutrient resorption, and water-use strategy, with leaf N concentration loading positively and leaf $\delta^{13}C$, *NRE*, and *PRE* loading negatively (Fig. 3A).

The two species showed contrasting multivariate differences between monocultures and mixed stands

(Fig. 3B). For *D. odorifera*, individuals in monocultures and mixed stands differed significantly along PC1 but not PC2, indicating that the differences between stand types were primarily associated with coordinated variation in structural and hydraulic traits. In contrast, *A. fraxinifolius* individuals differed significantly between stand types along PC2 but not PC1, indicating that these differences were primarily associated with variation in leaf N concentration, N and P resorption efficiencies, and leaf $\delta^{13}C$ (Fig. 3C–D).

Relationships between functional traits and demographic performance

Linear regression analyses of observations pooled across both species and stand types showed that annual DBH increment decreased significantly with increasing *PRE* (R^2 = 0.21, P = 0.040), *NRE* (R^2 = 0.44, P = 0.001), and $\delta^{13}C$ (R^2 = 0.67, P < 0.001; Fig. 4A–C). No significant relationship was detected between annual DBH increment and leaf N concentration (Fig. S2). Cumulative mortality recorded in 2024 decreased significantly with increasing Ψ_{min} (R^2 = 0.63, P < 0.001), *LMA* (R^2 = 0.70, P < 0.001), and HSM_{88} (R^2 = 0.79, P < 0.001; Fig. 4D–F). No significant relationship was detected between cumulative mortality and SWC_{stem} (Fig. S2).

Discussion

Contrasting growth and mortality responses of the two Fabaceae species between stand types

We found low cumulative mortality in the two tree species used for afforestation at the seedling stage (8 months after planting; mean = 10.75%) and the sapling stage (2 years after planting; mean = 15.15%) in both monocultures and mixed stand. Although three severe drought episodes (SPEI < −2) occurred between 2011 and 2023, cumulative mortality remained below 25% after 13 years (Fig. S3). These results indicated that these two Fabaceae species could successfully establish and persist in the KRD environment. By comparison, fast-growing pioneer tree species (e.g., *Acacia dealbata* and *Eucalyptus* spp.) planted in KRD area in Shilin, Yunnan

show a mean mortality of 25.1% following a single El Niño event (Yu et al. 2011). It should be note that *D. odorifera* is a non-karst tree species naturally distributed in tropical rain forests in southern China (Zhang et al. 2012). The successful establishment of *D. odorifera* therefore implies that non-karst tree species (from a same climatic region) can provide supplemental resources of tool tree species used for KRD restoration (Reisman-Berman et al. 2019; Pötzelsberger et al. 2020).

The two species exhibited contrasting demographic performance between monoculture and mixed stand: *D. odorifera* significantly decreased cumulative mortality in mixed stand, whereas *A. fraxinifolius* significantly increased growth (Fig. 2). Similar patterns have also been observed in many other timber plantations. For example, *P. quinata* in mixed stand with N-fixing tree species *Dalbergia retusa* had higher growth rates than in monoculture due to increased soil nutrient availability (Mayoral et al. 2017). In another study, the drought-induced mortality of European beech (*Fagus sylvatica*) was significantly lower in mixed stands with sessile oak (*Quercus petraea*) than in monoculture, because hydraulic lift by oak alleviates water stress in beech (Pretzsch et al. 2013). Taken together, these findings indicate that species-specific responses of growth and mortality enable mixed stands to improve their overall stability and productivity.

In the water- and nutrient-limited KRD area in the present study, the demographic responses to mixed planting may depend largely on whether changes in resource availability in their mixed stand alleviate the principal limitation of each species. At the same study site, previous studies have demonstrated that mixed stands can improve soil N and P availability relative to monocultures, potentially through enhanced soil microbial activity and nutrient cycling (Table 1; Li et al. 2022; Su et al. 2022; Zhang et al. 2022). *A. fraxinifolius* is a deep-rooted, generally fast-growing timber tree species (Nath et al. 2011; Araujo et al. 2022), exhibiting a more acquisitive strategy than *D. odorifera* (Fig. 3). Consequently, improved resource availability could promote growth in more acquisitive species but enhance persistence in more conservative species, as

species-specific resource-use strategies may determine whether improved resource conditions primarily support growth or alleviate hydraulic stress and mortality risk (Forrester and Bauhus, 2016; Grossiord, 2020). Although this study did not investigate root trait responses, previous pot-based simulation experiments have shown that the non-karst species *D. odorifera* exhibits significant root morphological plasticity in response to the KRD environment (Xiang et al. 2021a; Xiang et al. 2021b), which may facilitate its access to water stored in epikarst layer in the mixed stand. This could therefore alleviate the degree of drought stress and decrease cumulative drought-induced mortality. In addition, the two species differ markedly in stature and light requirements. *A. fraxinifolius* is a tall, light-demanding species, whereas *D. odorifera* generally has a smaller mature stature (Orwa et al. 2009; Zhang et al. 2022; Flora of China). Consistent with these differences, *A. fraxinifolius* attained a greater mean height than *D. odorifera* in the present mixed stands (15.90 vs. 11.40 m, respectively; Table 1). Such vertical canopy differentiations enable *A. fraxinifolius* to maintain effective light capture and *D. odorifera* (located in the mid-canopy layer) to reduce excessive evaporative water loss.

Mixed stands strengthen hydraulic safety in *D. odorifera* and promote a resource-acquisitive strategy in *A. fraxinifolius*

We found significant structural and hydraulic adjustments in *D. odorifera* in mixed stand (Fig. 2 and 3). Stem saturated water content was higher in mixed stands, which may help buffer the intense moisture fluctuations in karst environments (Meinzer et al. 2009; Poorter et al. 2009). Combined with its root morphological adjustments and reduced exposure to high irradiance (as discussed above), these factors could explain the improved water potential during drought periods. As P_{88} changed relatively little between stand types (Fig. S1), this led to a wider hydraulic safety margin for *D. odorifera* in the mixed stand. Given the fact that hydraulic failure is a key physiological mechanism triggering tree death (Anderegg et al. 2016; Duan et al. 2022) and HSM_{88} is a reliable predictor of drought-induced mortality rates (Wang et al. 2023), it is no

wonder that *D. odorifera* in mixed stand showed lower cumulative mortality than in monocultures (Fig. 5). These results support a recent view that hydraulic trait adjustment in response to altered water availability can enhance drought resistance (Smith-Martin et al. 2026).

By comparison, *A. fraxinifolius* exhibited a shift toward a more resource-acquisitive strategy in mixed stands, potentially in response to enhanced nutrient availability (Fig. 2 and 3). Similarly, when *Robinia pseudoacacia* was mixed with *Amygdalus davidiana* or *Armeniaca sibirica*, both *A. davidiana* and *A. sibirica* showed increased leaf N and P concentrations and reduced N and P resorption efficiencies, indicating reduced reliance on internal nutrient recycling and greater nutrient acquisition from the soil (Lu et al. 2025). Similar changes in carbon isotope composition have also been reported in mixed forests. For example, *Fagus sylvatica* exhibited more negative leaf $\delta^{13}C$ values in mixtures with *Abies alba* than in monocultures under relatively wet climatic conditions, consistent with a more resource-acquisitive strategy (Didion-Gency et al. 2021). The more negative $\delta^{13}C$ values found in our mixed stand may also reflect greater stomatal openness, potentially facilitating carbon acquisition (Seibt et al. 2008; Cernusak et al. 2013; Ma et al. 2021). Therefore, tree species with physiologically active, nutrient-rich leaves generally grow faster (Webb et al. 2000; Masuda et al. 2022).

Implications for karst restoration

First, developing precious timber plantations using ecologically suitable Fabaceae species may provide an effective way for long-term karst restoration, because short-rotation plantations managed for rapid biomass production may not be suitable in resource-limited karst environments. The abundant Fabaceae tree species in tropical and subtropical karst forests provide a broad pool of candidate species for KRD restoration, and non-karst Fabaceae species from climatically similar regions could also be considered. Second, functional traits related to hydraulic safety and nutrient-use strategies can help predict tree persistence and productivity in resource-limited karst environments, thus providing useful criteria for species selection and the design of

mixed stands. Importantly, plantation management should also consider intraspecific trait variation, as such adjustments may influence tree growth and survival. Controlled pot experiments that manipulate water availability, nutrient supply, and stand type could evaluate trait responses to changes in environmental conditions. Third, the hydraulic safety margin, a promising indicator of drought-induced mortality risk, may help assess the drought risks of plantations in KRD areas under climate change. At the study site, current plantations contained approximately 1400–1600 trees ha^{-1} with DBH ≥ 10 cm (Table 1), exceeding the typical tree density in natural karst forests (300–1000 trees ha^{-1}, DBH ≥ 10 cm; Tao et al. 2021). Thus, competition for limited water resources may intensify as stands develop. We recommend long-term monitoring of hydraulic safety and tree growth, which could inform plantation management, particularly the timing and intensity of thinning.

Conclusion

Our findings demonstrate species-specific responses to mixed planting in KRD areas, i.e., *D. odorifera* exhibits lower cumulative mortality associated with enhanced hydraulic safety, whereas *A. fraxinifolius* shows greater growth associated with a more resource-acquisitive strategy. These contrasting responses highlight the importance of species-specific functional trait adjustments when selecting tree combinations for the restoration of degraded karst landscapes. Trait-based species selection, together with appropriate stand management, may therefore help improve the long-term stability and productivity of plantations in KRD areas.

Authors' Contributions Chun-Yan Wan: Writing – review & editing, Writing – original draft, Visualization, Software, Data curation. Yuan-Guang Wen: Resources. Xiao-Guo Zhou: Resources. Shi-Dan Zhu: Writing – review & editing, Conceptualisation, Funding acquisition.

Funding This work was funded by the National Natural Science Foundation of China (32560337), the Guangxi Science and Technology Base and Talent Special Project (AD25069066), and the Natural Science Foundation of Guangxi Zhuang Autonomous Region (2023GXNSFFA026008).

Acknowledgments We sincerely thank Xu Han, Hongjia Wu, Feifei Fan, and Zaibing Zhang for their valuable assistance with the field collection of branch and leaf samples.

Data availability Data will be made available on request.

Declarations

Conflict of interest The authors declare that they have no competing interests.

References

Albert CH, Thuiller W, Yoccoz NG, et al. (2010) Intraspecific functional variability: extent, structure and sources of variation. J Ecol 98:604–613. https://doi.org/10.1111/j.1365-2745.2010.01651.x

Anderegg WRL, Klein T, Bartlett M, et al. (2016) Meta-analysis reveals that hydraulic traits explain cross-species patterns of drought-induced tree mortality across the globe. Proc Natl Acad Sci U S A 113:5024–5029. https://doi.org/10.1073/pnas.1525678113

Araujo G, de Almeida R, Vieira dos Santos L, et al. (2022) Initial development of *Acrocarpus fraxinifolius* in function of soil preparation and phosphate mineral fertilization. Floresta Ambient 29:e20210082. https://doi.org/10.1590/2179-8087-floram-2021-0082

Bucci SJ, Carbonell Silletta LM, Garré A, et al. (2019) Functional relationships between hydraulic traits and the timing of diurnal depression of photosynthesis. Plant Cell Environ 42:1603–1614. https://doi.org/10.1111/pce.13512

Busch FA, Holloway-Phillips M, Stuart-Williams H, et al. (2020) Revisiting carbon isotope discrimination in C3 plants shows respiration rules when photosynthesis is low. Nat Plants 6:245–258. https://doi.org/10.1038/s41477-020-0606-6

Cernusak LA, Ubierna N, Winter K, et al. (2013) Environmental and physiological determinants of carbon isotope discrimination in terrestrial plants. New Phytol 200:950–965. https://doi.org/10.1111/nph.12423

Chave J, Coomes D, Jansen S, et al. (2009) Towards a worldwide wood economics spectrum. Ecol Lett 12:351–366. https://doi.org/10.1111/j.1461-0248.2009.01285.x

Choat B, Jansen S, Brodribb TJ, et al. (2012) Global convergence in the vulnerability of forests to drought. Nature 491:752–755. https://doi.org/10.1038/nature11688

Da Silveira L, Sternberg L, Mulkey SS, et al. (1989) Ecological interpretation of leaf carbon isotope ratios: influence of respired carbon dioxide. Ecology 70:1317–1324. https://doi.org/10.2307/1938191

Delzon S, Cochard H (2014) Recent advances in tree hydraulics highlight the ecological significance of the hydraulic safety margin. New Phytol 203:355–358. https://doi.org/10.1111/nph.12798

Didion-Gency M, Bachofen C, Buchmann N, et al. (2021) Interactive effects of tree species mixture and climate on foliar and woody trait variation in a widely distributed deciduous tree. Funct Ecol 35:2397–2408. https://doi.org/10.1111/1365-2435.13898

Driscoll AW, Bitter NQ, Sandquist DR, et al. (2020) Multidecadal records of intrinsic water-use efficiency in the desert shrub *Encelia farinosa* reveal strong responses to climate change. Proc Natl Acad Sci U S A 117:18161–18168. https://doi.org/10.1073/pnas.2008345117

Duan H, Resco de Dios V, Wang D, et al. (2022) Testing the limits of plant drought stress and subsequent recovery in four provenances of a widely distributed subtropical tree species. Plant Cell Environ 45:1187–1203. https://doi.org/10.1111/pce.14254

Díaz S, Kattge J, Cornelissen JHC, et al. (2016) The global spectrum of plant form and function. Nature 529:167–171. https://doi.org/10.1038/nature16489

Felix JA, Stevenson PC, Koricheva J (2023) Plant neighbourhood diversity effects on leaf traits: a meta-analysis. Funct Ecol 37:3150–3163. https://doi.org/10.1111/1365-2435.14441

Feng X, Zhong L, Tian Q, et al. (2022) Leaf water potential-dependent leaflet closure contributes to legume leaves cool down and drought avoidance under diurnal drought stress. Tree Physiol 42:2239–2251. https://doi.org/10.1093/treephys/tpac075

Fichtner A, Härdtle W, Bruelheide H, et al. (2018) Neighbourhood interactions drive overyielding in mixed-species tree communities. Nat Commun 9:1144. https://doi.org/10.1038/s41467-018-03529-w

Forrester DI, Bauhus J (2016) A review of processes behind diversity—productivity relationships in forests. Curr For Rep 2:45–61. https://doi.org/10.1007/s40725-016-0031-2

Forrester DI, Bauhus J, Cowie AL (2005) Nutrient cycling in a mixed-species plantation of *Eucalyptus globulus* and *Acacia mearnsii*. Can J For Res 35:2942–2950. https://doi.org/10.1139/x05-214

Griffin-Nolan RJ, Chieppa J, Knapp AK, et al. (2023) Coordination of hydraulic and morphological traits across dominant grasses in eastern Australia. Funct Ecol 37:1126–1139. https://doi.org/10.1111/1365-2435.14283

Grossiord C (2020) Having the right neighbors: how tree species diversity modulates drought impacts on forests. New Phytol 228:42–49. https://doi.org/10.1111/nph.15667

Guimarães ZTM, Coelho-Silva D, Soares JCR, et al. (2026) Interspecific variation of functional traits in saplings of three Amazonian species under drought stress and recovery. AoB Plants 18:plaf073. https://doi.org/10.1093/aobpla/plaf073

He Y, Wang L, Niu Z, et al. (2022) Vegetation recovery and recent degradation in different karst landforms of southwest China over the past two decades using GEE satellite archives. Ecol Inform 68:101555. https://doi.org/10.1016/j.ecoinf.2022.101555

Jiang Z, Lian Y, Qin X (2014) Rocky desertification in southwest China: impacts, causes, and restoration. Earth Sci Rev 132:1–12. https://doi.org/10.1016/j.earscirev.2014.01.005

Kettle CJ (2012) Seeding ecological restoration of tropical forests: priority setting under REDD+. Biol Conserv 154:34–41. https://doi.org/10.1016/j.biocon.2012.03.016

Killingbeck KT (1996) Nutrients in senesced leaves: keys to the search for potential resorption and resorption

proficiency. Ecology 77:1716–1727. https://doi.org/10.2307/2265777
Kunstler G, Falster D, Coomes DA, et al. (2016) Plant functional traits have globally consistent effects on competition. Nature 529:204–207. https://doi.org/10.1038/nature16476
Li J, Prentice IC (2024) Global patterns of plant functional traits and their relationships to climate. Commun Biol 7:1136. https://doi.org/10.1038/s42003-024-06777-3
Li M, You Y, Tan X, et al. (2022) Mixture of N2-fixing tree species promotes organic phosphorus accumulation and transformation in topsoil aggregates in a degraded karst region of subtropical China. Geoderma 413:115752. https://doi.org/10.1016/j.geoderma.2022.115752
Li Y, Wang S, Peng T, et al. (2023) Hydrological characteristics and available water storage of typical karst soil in SW China under different soil–rock structures. Geoderma 438:116633. https://doi.org/10.1016/j.geoderma.2023.116633
Liu C, Liu Y, Guo K, et al. (2018) Effects of nitrogen, phosphorus and potassium addition on the productivity of a karst grassland: plant functional group and community perspectives. Ecol Eng 117:84–95. https://doi.org/10.1016/j.ecoleng.2018.04.008
Lu S, Chen Y, Sardans J, et al. (2025) Impact of mixed plantation strategies on the nutrient concentrations of green and senescent leaves and their nutrient resorption efficiencies in temperate forests of the Loess Hilly Region. Front Plant Sci 16:1527930. https://doi.org/10.3389/fpls.2025.1527930
Luo Y, Ho C, Helliker B, et al. (2021) Leaf water storage and robustness to intermittent drought: a spatially explicit capacitive model for leaf hydraulics. Front Plant Sci 12:725995. https://doi.org/10.3389/fpls.2021.725995
Ma WT, Tcherkez G, Wang XM, Schäufele R, Schnyder H, Yang Y, Gong XY (2021) Accounting for mesophyll conductance substantially improves ^{13}C-based estimates of intrinsic water-use efficiency. New Phytol 229:1326–1338. https://doi.org/10.1111/nph.16958
Ma WT, Yu YZ, Wang X, Gong XY (2023) Estimation of intrinsic water-use efficiency from $\delta^{13}C$ signature of C3 leaves: assumptions and uncertainty. Front Plant Sci 13:1037972. https://doi.org/10.3389/fpls.2022.1037972
Masuda C, Morikawa Y, Masaka K, et al. (2022) Hardwood mixture increases stand productivity through increasing the amount of leaf nitrogen and modifying biomass allocation in a conifer plantation. For Ecol Manage 504:119835. https://doi.org/10.1016/j.foreco.2021.119835
Matos IS, Boakye M, Niewiadomski I, et al. (2024) Leaf venation network architecture coordinates functional trade-offs across vein spatial scales: evidence for multiple alternative designs. New Phytol 244:407–425. https://doi.org/10.1111/nph.20037
Mayoral C, van Breugel M, Cerezo A, et al. (2017) Survival and growth of five neotropical timber species in monocultures and mixtures. For Ecol Manage 403:1–11. https://doi.org/10.1016/j.foreco.2017.08.002
Meinzer FC, Johnson DM, Lachenbruch B, et al. (2009) Xylem hydraulic safety margins in woody plants: coordination of stomatal control of xylem tension with hydraulic capacitance. Funct Ecol 23:922–930. https://doi.org/10.1111/j.1365-2435.2009.01577.x
Menge DNL, Hedin LO (2009) Nitrogen fixation in different biogeochemical niches along a 120 000-year chronosequence in New Zealand. Ecology 90:2190–2201. https://doi.org/10.1890/08-0877.1
Nath C, Pélissier R, Ramesh B, et al. (2011) Promoting native trees in shade coffee plantations of southern India: comparison of growth rates with the exotic *Grevillea robusta*. Agrofor Syst 83:107–119. https://doi.org/10.1007/s10457-011-9401-8
Nolf M, Creek D, Duursma R, et al. (2015) Stem and leaf hydraulic properties are finely coordinated in three tropical rain forest tree species. Plant Cell Environ 38:2652–2661. https://doi.org/10.1111/pce.12581

526 Orwa C, Mutua A, Kindt R, Jamnadass R, Simons A (2009) Agroforestree database: a tree reference and
527 selection guide, version 4.0. World Agroforestry Centre.
528 https://www.worldagroforestry.org/output/agroforestree-database. Accessed 26 October 2026
529 Pereira SR, Laura VA, Souza ALT (2013) Establishment of *Fabaceae tree* species in a tropical pasture:
530 influence of seed size and weeding methods. Restor Ecol 21:67–74. https://doi.org/10.1111/j.1526-
531 100X.2011.00858.x
532 Pineda-García F, Paz H, Meinzer FC (2013) Drought resistance in early and late secondary successional species
533 from a tropical dry forest: the interplay between xylem resistance to embolism, sapwood water storage
534 and leaf shedding. Plant Cell Environ 36:405–418. https://doi.org/10.1111/j.1365-3040.2012.02582.x
535 Poorter H, Niinemets Ü, Poorter L, et al. (2009) Causes and consequences of variation in leaf mass per area
536 (LMA): a meta-analysis. New Phytol 182:565–588. https://doi.org/10.1111/j.1469-8137.2009.02830.x
537 Pretzsch H, Schütze G, Uhl E (2013) Resistance of European tree species to drought stress in mixed versus
538 pure forests: evidence of stress release by inter-specific facilitation. Plant Biol 15:483–495.
539 https://doi.org/10.1111/j.1438-8677.2012.00670.x
540 Pérez-Ramos IM, Matías L, Gómez-Aparicio L, et al. (2019) Functional traits and phenotypic plasticity
541 modulate species coexistence across contrasting climatic conditions. Nat Commun 10:2555.
542 https://doi.org/10.1038/s41467-019-10453-0
543 Pötzelsberger E, Spiecker H, Neophytou C, et al. (2020) Growing non-native trees in European forests brings
544 benefits and opportunities but also has its risks and limits. Curr For Rep 6:339–353.
545 https://doi.org/10.1007/s40725-020-00129-0
546 Qiu S, Peng J, Zheng H, et al. (2022) How can massive ecological restoration programs interplay with social-
547 ecological systems? A review of research in the south China karst region. Sci Total Environ 807:150723.
548 https://doi.org/10.1016/j.scitotenv.2021.150723
549 Reisman-Berman O, Keasar T, Tel-Zur N (2019) Native and non-native species for dryland afforestation:
550 bridging ecosystem integrity and livelihood support. Ann For Sci 76:114. https://doi.org/10.1007/s13595-
551 019-0903-2
552 Sack L, Cowan PD, Jaikumar N, et al. (2003) The 'hydrology' of leaves: co-ordination of structure and function
553 in temperate woody species. Plant Cell Environ 26:1343–1356. https://doi.org/10.1046/j.0016-
554 8025.2003.01058.x
555 Salomón RL, Puértolas J, Miranda JC, et al. (2024) Nearly instantaneous stem diameter response to
556 fluctuations in the atmospheric water demand. Tree Physiol 44:tpae116.
557 https://doi.org/10.1093/treephys/tpae116
558 Scoffoni C, Chatelet DS, Pasquet-Kok J, et al. (2016) Hydraulic basis for the evolution of photosynthetic
559 productivity. Nat Plants 2:16072. https://doi.org/10.1038/nplants.2016.72
560 Seibt U, Rajabi A, Griffiths H, et al. (2008) Carbon isotopes and water use efficiency: sense and sensitivity.
561 Oecologia 155:441–454. https://doi.org/10.1007/s00442-007-0932-7
562 Serrano-León H, Nitschke R, Scherer-Lorenzen M, et al. (2022) Intra-specific leaf trait variability of *F.*
563 *sylvatica*, *Q. petraea* and *P. abies* in response to inter-specific competition and implications for forest
564 functioning. Tree Physiol 42:253–272. https://doi.org/10.1093/treephys/tpab109
565 Siefert A, Violle C, Chalmandrier L, et al. (2015) A global meta-analysis of the relative extent of intraspecific
566 trait variation in plant communities. Ecol Lett 18:1406–1419. https://doi.org/10.1111/ele.12508
567 Smith-Martin CM, Muscarella R, Brodribb TJ, et al. (2026) Species intraspecific variation drives tropical forest
568 drought resistance. Nature 657:164–169. https://doi.org/10.1038/s41586-026-10870-4
569 Sperry JS, Donnelly JR, Tyree MT (1988) A method for measuring hydraulic conductivity and embolism in

xylem. Plant Cell Environ 11:35–40. https://doi.org/10.1111/j.1365-3040.1988.tb01774.x
Su J, Zheng W, Gou X, et al. (2026) Bedrock lithology determines forest demographic responses to drought. Nat Commun 17:8574. https://doi.org/10.1038/s41467-026-76754-3
Su X, Gao G, Huang X, et al. (2022) Vegetation restoration with mixed N2-fixer tree species alleviates microbial C and N limitation in surface soil aggregates in south subtropical karst area, China. Forests 13:1701. https://doi.org/10.3390/f13101701
Sun S, Zeng X, Zhang D, et al. (2015) Diverse fungi associated with partial irregular heartwood of *Dalbergia odorifera*. Sci Rep 5:8464. https://doi.org/10.1038/srep08464
Tao S, Labrière N, Calders K, et al. (2021) Mapping tropical forest trees across large areas with lightweight cost-effective terrestrial laser scanning. Ann For Sci 78:103. https://doi.org/10.1007/s13595-021-01113-9
Torres-Ruiz JM, Cochard H, Delzon S, et al. (2024) Plant hydraulics at the heart of plant, crops and ecosystem functions in the face of climate change. New Phytol 241:984–999. https://doi.org/10.1111/nph.19463
Turcotte MM, Levine JM (2016) Phenotypic plasticity and species coexistence. Trends Ecol Evol 31:803–813. https://doi.org/10.1016/j.tree.2016.07.013
Urli M, Porté AJ, Cochard H, et al. (2013) Xylem embolism threshold for catastrophic hydraulic failure in angiosperm trees. Tree Physiol 33:672–683. https://doi.org/10.1093/treephys/tpt030
Vergutz L, Manzoni S, Porporato A, et al. (2012) Global resorption efficiencies and concentrations of carbon and nutrients in leaves of terrestrial plants. Ecol Monogr 82:205–220. https://doi.org/10.1890/11-0416.1
Wang C, Liu H, Zhu L, et al. (2021) Which traits are necessary to quickly select suitable plant species for ecological restoration? Ecological Solutions and Evidence 2:e12102. https://doi.org/10.1002/2688-8319.12102
Wang SJ, Liu QM, Zhang DF (2004) Karst rocky desertification in southwestern China: geomorphology, landuse, impact and rehabilitation. Land Degrad Dev 15:115–121. https://doi.org/10.1002/ldr.592
Wang Y, Song H, Chen Y, et al. (2023) Hydraulic determinants of drought-induced tree mortality and changes in tree abundance between two tropical forests with different water availability. Agric For Meteorol 331:109329. https://doi.org/10.1016/j.agrformet.2023.109329
Webb MJ, Reddell P, Hambleton A, et al. (2000) Growth response of four tropical plantation timber species to increasing phosphorus supply and assessment of phosphorus requirements using foliar analysis. New For 20:193–211. https://doi.org/10.1023/A:1006756105284
Westerband AC, Funk JL, Barton KE (2021) Intraspecific trait variation in plants: a renewed focus on its role in ecological processes. Ann Bot 127:397–410. https://doi.org/10.1093/aob/mcab011
Williamson GB, Wiemann MC (2010) Measuring wood specific gravity correctly. Am J Bot 97:519–524. https://doi.org/10.3732/ajb.0900243
Wright IJ, Reich PB, Westoby M, et al. (2004) The worldwide leaf economics spectrum. Nature 428:821–827. https://doi.org/10.1038/nature02403
Xiang L, Miao L, Yang F (2021a) Drought and nitrogen application modulate the morphological and physiological responses of *Dalbergia odorifera* to different niche neighbors. Front Plant Sci 12:664122. https://doi.org/10.3389/fpls.2021.664122
Xiang L, Miao L, Yang F (2021b) Neighbors, drought, and nitrogen application affect the root morphological plasticity of *Dalbergia odorifera*. Front Plant Sci 12:650616. https://doi.org/10.3389/fpls.2021.650616
Yang Q, Chen J, Yang G, et al. (2025) Dynamic evolution of rocky desertification and vegetation restoration and analysis of driving forces in southwest karst region from 2000 to 2020. PLoS One 20:e0332644. https://doi.org/10.1371/journal.pone.0332644

Yao G, Nie Z, Turner NC, et al. (2021) Combined high leaf hydraulic safety and efficiency provides drought tolerance in *Caragana species* adapted to low mean annual precipitation. New Phytol 229:230–244. https://doi.org/10.1111/nph.16845

Yu X, Li Y, Huang J, Li C, Li C, Duan W (2011) Impacts of extreme drought in spring 2010 on karst vegetations in Shilin of Yunnan Province, China. Chinese J Ecol 30:1441–1448. https://doi.org/10.13292/j.1000-4890.2011.0192

Yue Y, Qi X, Wang K, et al. (2022) Large scale rocky desertification reversal in south China karst. Prog Phys Geogr 46:661–675. https://doi.org/10.1177/03091333221083111

Yue Y, Wang L, Brandt M, et al. (2024) A social-ecological framework to enhance sustainable reforestation under geological constraints. Earths Future 12:e2023EF004335. https://doi.org/10.1029/2023EF004335

Zhang S, Landuyt D, Verheyen K, et al. (2022) Tree species mixing can amplify microclimate offsets in young forest plantations. J Appl Ecol 59:1428–1439. https://doi.org/10.1111/1365-2664.14158

Zhang S, Song Y, Wen H, et al. (2024) Leaf nitrogen and phosphorus resorption efficiencies are related to drought resistance across woody species in a Chinese savanna. Tree Physiol 44:tpad149. https://doi.org/10.1093/treephys/tpad149

Zhang W, Zhao J, Pan F, et al. (2015) Changes in nitrogen and phosphorus limitation during secondary succession in a karst region in southwest China. Plant Soil 391:77–91. https://doi.org/10.1007/s11104-015-2406-8

Zhang Y, Chen HYH, Reich PB (2012) Forest productivity increases with evenness, species richness and trait variation: a global meta-analysis. J Ecol 100:742–749. https://doi.org/10.1111/j.1365-2745.2011.01944.x

Zhang Y, Zhou X, Wen Y, et al. (2022) Characteristics of soil microbial community structure of three plantations in a karst region. Guihaia 42:938–950. https://doi.org/10.11931/guihaia.gxzw202102020

Zhao L, Hou R (2019) Human causes of soil loss in rural karst environments: a case study of Guizhou, China. Sci Rep 9:3225. https://doi.org/10.1038/s41598-018-35808-3

Zhong F, Xu X, Li Z, et al. (2022) Relationships between lithology, topography, soil, and vegetation, and their implications for karst vegetation restoration. Catena 209:105831. https://doi.org/10.1016/j.catena.2021.105831

Zhu S, He P, Li R, et al. (2018) Drought tolerance traits predict survival ratio of native tree species planted in a subtropical degraded hilly area in south China. For Ecol Manage 418:41–46. https://doi.org/10.1016/j.foreco.2017.09.016

Ziegler C, Coste S, Stahl C, et al. (2019) Large hydraulic safety margins protect neotropical canopy rainforest tree species against hydraulic failure during drought. Ann For Sci 76:115. https://doi.org/10.1007/s13595-019-0905-0

Tables

Table 1. Descriptions of the experimental plots. DO-Mono, *Dalbergia odorifera* monoculture; AF-Mono, *Acrocarpus fraxinifolius* monoculture; Mixed stands, mixed plantation of *A. fraxinifolius* and *D. odorifera*. Except for slope, other data are shown as means ± SE.

Table 2. Abbreviations, units, and definitions of functional traits.

Figure legends

Fig. 1 Location of the study area and representative stand types. (A) Karst landforms distribute extensively in eight provinces (left; blue areas) in Southwest China. The right map shows Guangxi Province, with grey shading representing karst regions and the red dot indicating the study site. **(B)** Photo of the study site before restoration in 2010. **(C)** *Dalbergia odorifera* monoculture. **(D)** *Acrocarpus fraxinifolius* monoculture. **(E)** Mixed stand of *Dalbergia odorifera* and *Acrocarpus fraxinifolius* (1:1).

Fig. 2 Effects of stand type on functional traits, growth, and cumulative mortality of *Acrocarpus fraxinifolius* and *Dalbergia odorifera*. Standardized effect sizes were calculated as the differences between mixed stands and monocultures (Mix − Mono), with positive values indicating higher values in mixed stands and negative values indicating lower values in mixed stands. Points represent standardized effect sizes, and horizontal error bars indicate 95% confidence intervals. Red and blue points indicate significant positive and negative effects, respectively, whereas gray points indicate non-significant effects. *, $P < 0.05$; **, $P < 0.01$; ***, $P < 0.001$. Growth represents annual DBH increment, whereas cumulative mortality represents the proportion of trees that died since plantation establishment. Trait abbreviations are shown in Table 2.

671

672 **Fig. 3 Principal component analysis (PCA) of functional traits in *Acrocarpus fraxinifolius* (AF) and**
673 ***Dalbergia odorifera* (DO) from monocultures and mixed stand. (A)** PCA loading plot showing the
674 directions and contributions of functional traits to the first two principal components. **(B)** PCA score plot
675 showing the distribution of plot-level observations among AF-Mix, AF-Mono, DO-Mix, and DO-Mono groups.
676 Each point represents one plot-level observation (n = 5 plots per species × stand-type combination), and
677 polygons indicate the distribution of observations within each group. Comparisons of **(C)** PC 1 and **(D)** PC 2
678 scores between stand types for each species. Asterisks indicate significant differences ($P < 0.05$), whereas ns
679 indicates no significant difference. Trait abbreviations are shown in Table 2.

680

681 **Fig. 4 Relationships of functional traits with annual DBH increment and cumulative mortality.** Gray
682 points represent plot-level observations, whereas colored symbols represent group means for each species ×
683 stand-type combination. Error bars indicate variation around group means. Solid regression lines indicate
684 significant relationships, and gray shaded areas indicate 95% confidence intervals. Regression equations,
685 coefficients of determination (R^2), and significance levels (P) are shown in each panel. Trait abbreviations are
686 shown in Table 2.

687 **Fig. 5 Conceptual illustration of species-specific functional trait adjustments in *Dalbergia odorifera* and**
688 ***Acrocarpus fraxinifolius* in mixed stands relative to monocultures.** The diagram illustrates differences in
689 hydraulic safety and nutrient-use strategies between stand types and their associations with growth and
690 cumulative mortality. Soil water and nutrient availability represent potential belowground factors contributing
691 to these differences. Widening green and narrowing blue triangles indicate increases and decreases in trait
692 values in mixed stands relative to monocultures, respectively. Trait abbreviations are shown in Table 2.

693 **Table 1**

Stand type	Soil water content (%)	Nitrate nitrogen (mg kg^{-1})	Available P (mg kg^{-1})	Canopy cover (%)	Slope (°)	Density (trees ha^{-1})	DBH (cm)	Height (m)	Basal Area (m^2 ha^{-1})
DO-Mono	33.75 ± 6.21	19.39± 0.81	7.07± 0.70	61.58 ± 6.35	20–30	1338 ± 75	10.94 ± 0.14	10.56 ± 0.10	14.98 ± 0.35
AF-Mono	36.64 ± 5.33	28.18± 2.52	11.10± 1.26	55.42 ± 4.52	25–30	1084 ± 102	13.21 ± 0.17	13.42 ± 0.32	14.88 ± 0.38
Mixed stand	39.35 ± 4.20	34.17± 3.67	18.01± 0.64	60.12 ± 5.35	25–35	1279 ± 189	13.37 ± 0.18	13.52 ± 0.20	18.21 ± 0.52

694

695

Table 2

Traits	Code	Unit	Definition
Leaf mass per area	LMA	$g \cdot m^{-2}$	Defined as leaf dry mass per unit area. A central leaf economic trait that is related to carbon investment
Leaf saturated water content	SWC_{leaf}	$g\ g^{-1}$	Water content of fully hydrated leaves, calculated from saturated mass and dry mass. It reflects leaf water storage capacity and drought-buffering ability.
Stem saturated water content	SWC_{stem}	$g\ g^{-1}$	Water content of fully hydrated stem tissues, calculated from saturated mass and dry mass. It indicates stem water storage capacity and potential buffering against short-term drought stress.
Wood density	WD	$g\ cm^{-3}$	Stem dry mass per unit fresh volume. It reflects carbon investment in woody tissues, mechanical support, and hydraulic construction strategy.
Leaf cavitation resistance	$P88_{leaf}$	MPa	Defined as the water potential inducing 88% loss of leaf hydraulic conductance. It reflects embolic resistance and the threshold of hydraulic failure
Leaf hydraulic conductance	K_{leaf}	$mmol \cdot m^{-2} \cdot s^{-1} \cdot MPa^{-1}$	Leaf water transport capacity per unit leaf area under hydrated conditions. It reflects the efficiency of water supply from petiole to leaf lamina.
Stem cavitation resistance	$P88_{stem}$	MPa	Water potential inducing 88% loss of stem hydraulic conductivity. More negative values indicate stronger resistance to xylem embolism and stem hydraulic failure.
Stem hydraulic conductivity	K_{stem}	$kg\ m^{-1}\ s^{-1}\ MPa^{-1}$	Water transport efficiency of stem xylem. It reflects the capacity of stems to conduct water from roots to leaves.
Hydraulic safety margin	HSM_{88}	MPa	Difference between minimum leaf water potential and $P88_{stem}$. It indicates the safety buffer between actual plant water status and the threshold of severe hydraulic dysfunction.
Nitrogen per unit dry mass	N	$mg\ g^{-1}$	Leaf nitrogen concentration per unit dry mass. It reflects plant nitrogen status, photosynthetic capacity, and nutrient acquisition strategy.
Phosphorus per unit dry mass	P	$mg\ g^{-1}$	Leaf phosphorus concentration per unit dry mass. It indicates phosphorus availability, metabolic activity, and potential phosphorus limitation.
Calcium per unit dry mass	Ca	$mg\ g^{-1}$	Leaf calcium concentration per unit dry mass. It reflects calcium accumulation, ion regulation, and adaptation to high-calcium karst soils.
Magnesium per unit dry mass	Mg	$mg\ g^{-1}$	Leaf magnesium concentration per unit dry mass. It is closely related to chlorophyll formation, photosynthesis, and enzymatic activity.
Carbon isotope composition	$\delta^{13}C$	‰	Stable carbon isotope composition of leaves. It is commonly used as an integrated indicator of stomatal regulation and intrinsic water-use efficiency.
Nitrogen resorption efficiency	NRE	%	Proportion of nitrogen withdrawn from leaves before senescence. It reflects the capacity of plants to conserve nitrogen and reduce dependence on external nitrogen supply.

Phosphorus resorption efficiency	PRE	%	Proportion of phosphorus withdrawn from leaves before senescence. It reflects phosphorus conservation capacity and adaptation to phosphorus-limited environments.
Growth rate	Growth	cm yr^{-1}	Defined as the annual increment in diameter at breast height during the observation period. It reflects individual tree growth performance and resource acquisition capacity under different planting modes.
Cumulative mortality	Cumulative mortality	%	Proportion of dead individuals during the observation period. It reflects plantation survival status and tree tolerance to environmental stress.

697

698 **Fig. 1**

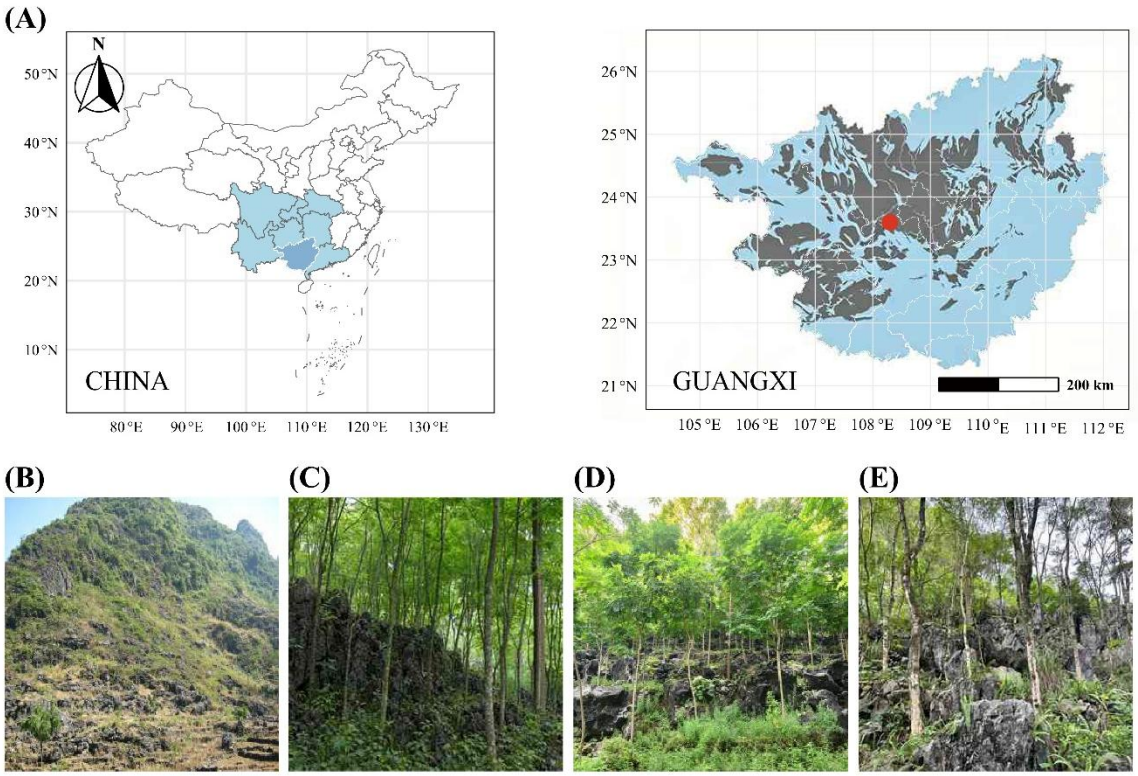

699

700

701 **Fig. 2**

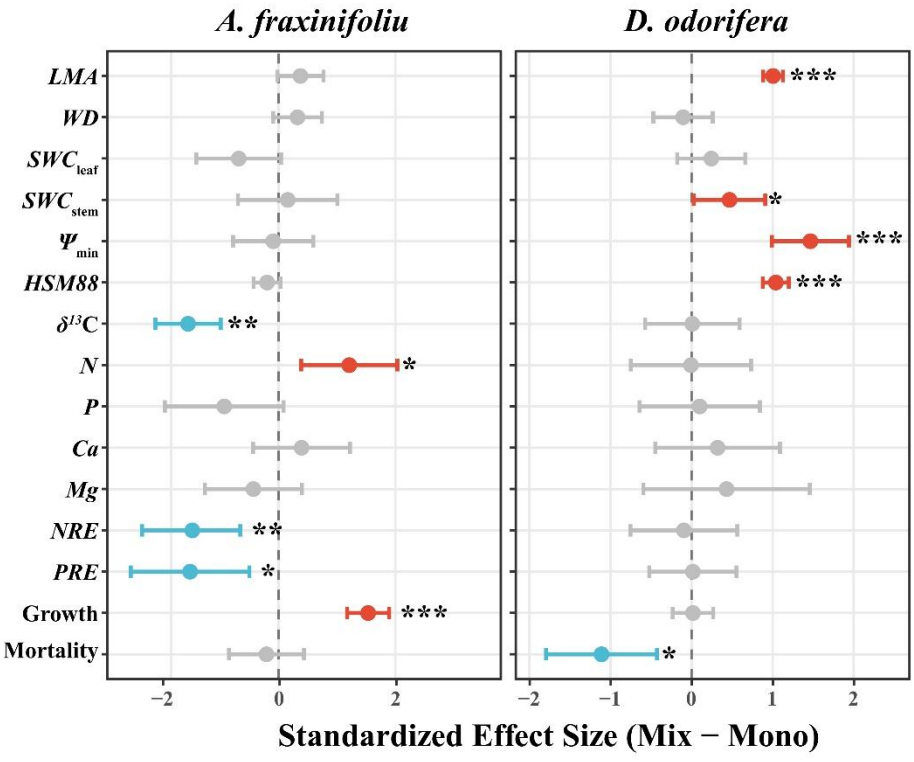

702

703 **Fig. 3**

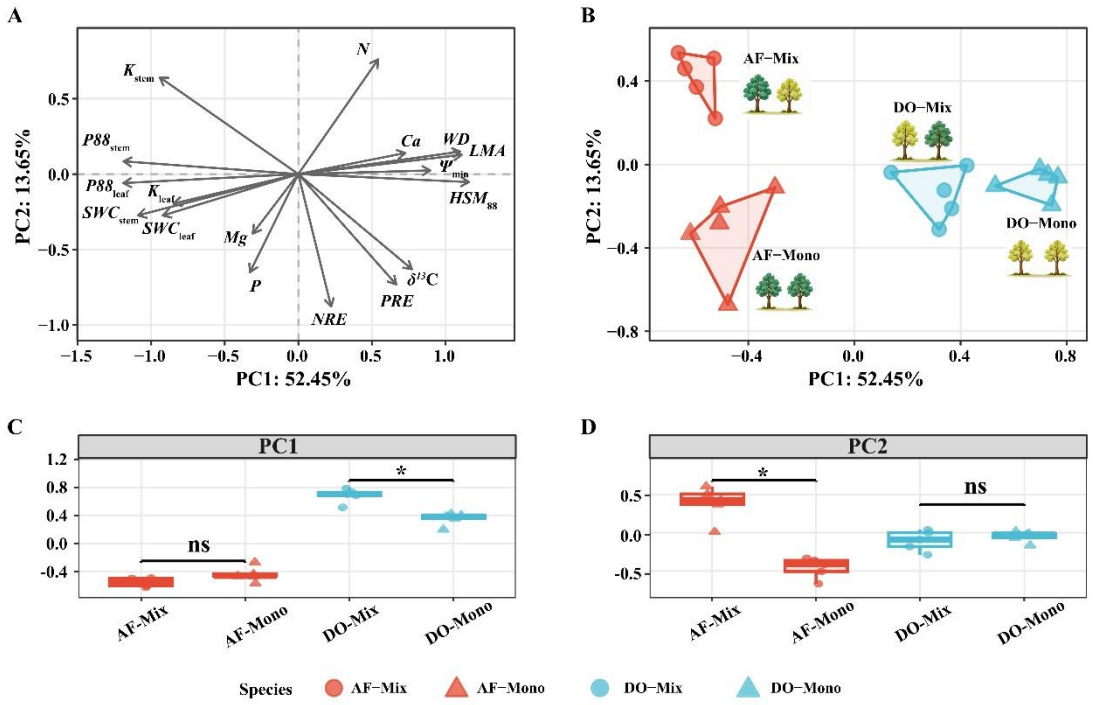

704

705

706 **Fig. 4**

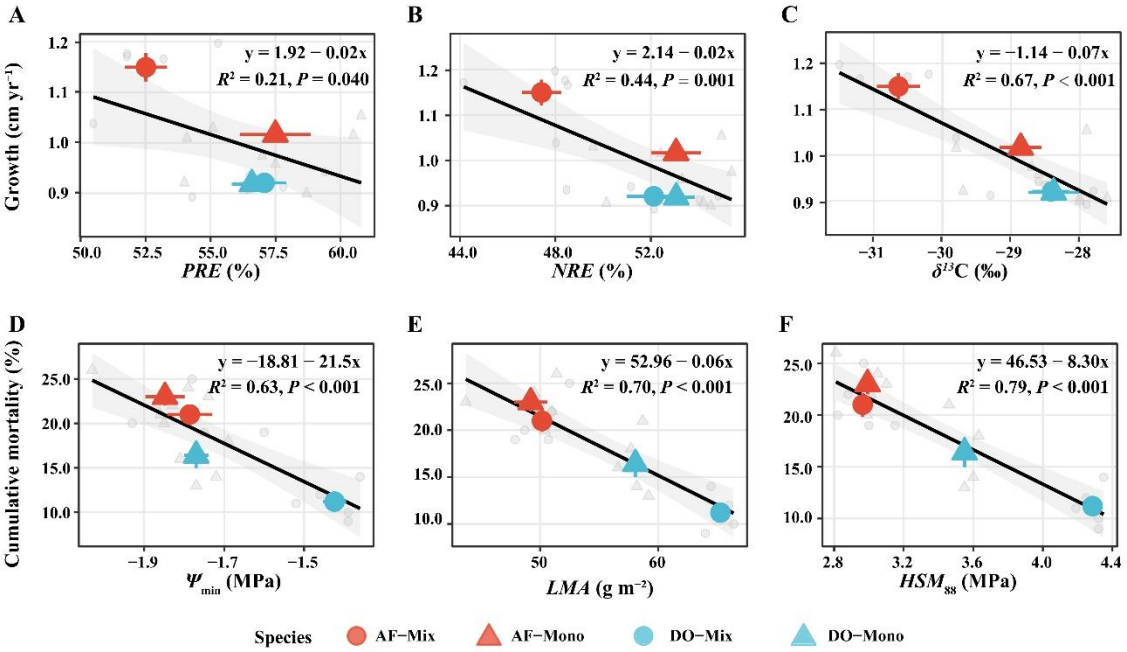

707

708 **Fig. 5**

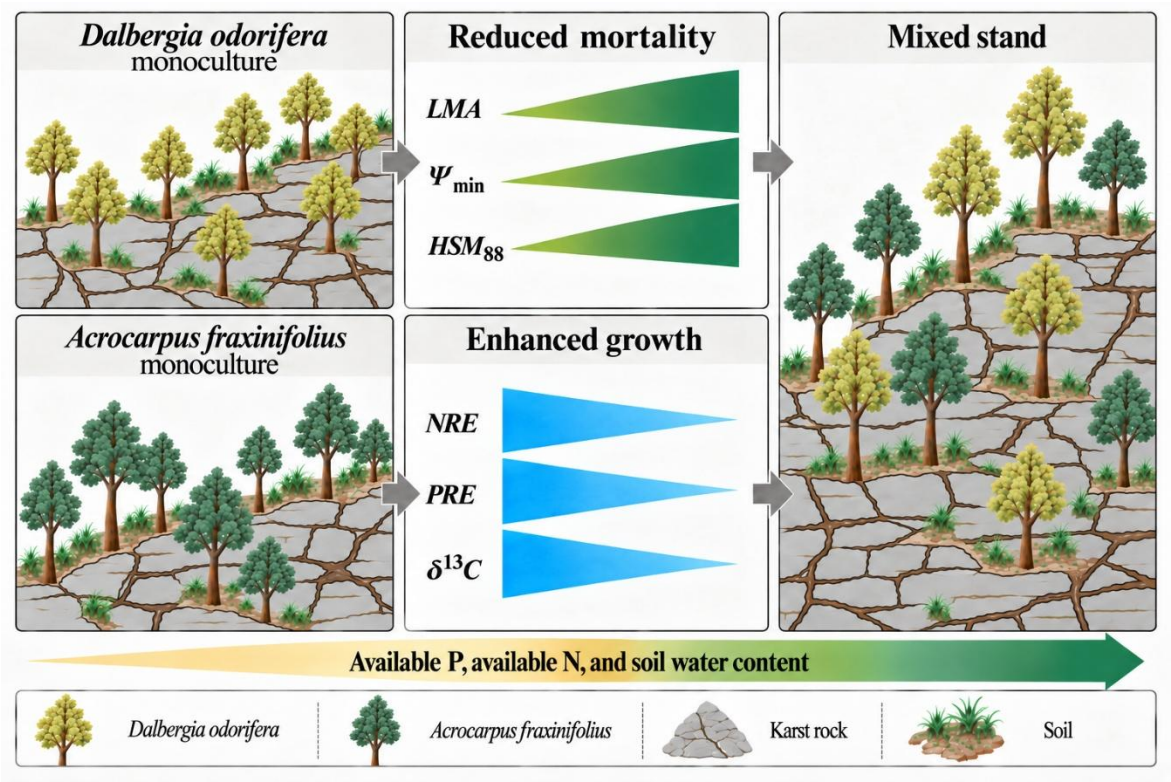
Dalbergia odorifera
monoculture
Reduced mortality
LMA
Ψ min
HSM88
Mixed stand
Acrocarpus fraxinifolius
monoculture
Enhanced growth
NRE
PRE
δ13C
Available P, available N, and soil water content
Dalbergia odorifera
Acrocarpus fraxinifolius
Karst rock
Soil

709

Supplementary Files

This is a list of supplementary files associated with this preprint. Click to download.

- SupplementaryMaterial.docx